Struct Multidisc Optim (2010) 40:77–96
DOI 10.1007/s00158-009-0372-6

RESEARCH PAPER

Optimal uncertainty reduction for multi-disciplinary multi-output systems using sensitivity analysis

M. Li · J. Hamel · S. Azarm

Received: 19 August 2008 / Revised: 30 December 2008 / Accepted: 12 February 2009 / Published online: 9 April 2009

Abstract We present a sensitivity analysis based uncertainty reduction approach, called Multi-dIsciplinary Multi-Output Sensitivity Analysis (MIMOSA), for the analysis model of a multi-disciplinary engineering system decomposed into multiple subsystems with each subsystem analysis having multiple inputs with reducible uncertainty and multiple outputs. MIMOSA can determine: (1) the sensitivity of system and subsystem outputs to input uncertainties at both system and subsystem levels, (2) the sensitivity of the system outputs to the variation from subsystem outputs, and (3) the optimal "investment" required to reduce uncertainty in inputs in order to obtain a maximum reduction in output variations at both the system and subsystem levels. A numerical and an engineering example with two and three subsystems, respectively, have been used to demonstrate the applicability of the MIMOSA approach.

Keywords Uncertainty reduction · Sensitivity analysis · Multi-disciplinary analysis · Interval uncertainty

M. Li · J. Hamel · S. Azarm (✉)
Department of Mechanical Engineering,
University of Maryland, College Park,
MD 20742, USA
e-mail: azarm@umd.edu

M. Li
e-mail: mli6@umd.edu

J. Hamel
e-mail: hamel@umd.edu

Nomenclature

i	index of subsystems
K	Dimension of parameters
$\boldsymbol{o}$	vector of outputs
$\boldsymbol{p}$	vector of parameters
$\boldsymbol{t}$	vector of target variables
$\boldsymbol{x}$	vector of design variables
$\boldsymbol{y}$	vector of coupling variables
$\boldsymbol{Y}$	functions to calculate the coupling variables
SS0	System level optimization problem
SSi	SubSystem i
α	Parameter Uncertainty Reduction Index (*PURI*)

1 Introduction

This paper presents a new global sensitivity analysis approach that can be used for the sensitivity analysis of multi-subsystem multi-output analysis models in engineering design problems in which the inputs to the analysis subsystems have reducible uncertainty. This new approach is called: *M*ulti-d*I*sciplinary *M*ulti-*O*utput *S*ensitivity *A*nalysis (MIMOSA). MIMOSA has several key properties and capabilities: (a) it quantifies variation in multiple outputs in the system and/or each subsystem with respect to input interval uncertainty, considering multiple uncertain input parameters for a single design or a set of designs; (b) it identifies the uncertain parameters, at the system and subsystem levels, which have the greatest effect on system output variations; and (c) it does not require gradient information or probability density functions to quantify the uncertain parameters, rather it uses interval uncertainty which is more flexible and easier to obtain or estimate.

In the context Multi-Disciplinary Optimization (MDO), there have been numerous approaches proposed in the literature for ensuring that optimal design solutions are insensitive to the uncertainty associated with the system's input parameters, mostly in the area of robust optimization (e.g., Du and Chen 2002, 2005; Agarwal et al. 2004; Smith and Mahadevan 2005; Kokkolaras et al. 2006; Padula et al. 2006; Gu et al. 2006; Chiralaksanakul and Mahadevan 2007; Li and Azarm 2008). Those approaches, while valuable, do not address the possibility that in some cases the uncertainty in a system or its corresponding subsystems could be reduced to some level given enough investment and that reduction in uncertainty could in turn improve both the system's and its corresponding subsystems' performance without the need for additional design optimization. This fact drives the need for a better understanding of the nature and effects of uncertainty in multi-disciplinary systems. Such knowledge would also lead to a better understanding of uncertainty, the relative importance of particular parameters and the opportunities to systematically apply limited resources in order to reduce the variations in a system's outputs optimally. Sensitivity Analysis (SA) techniques provide a particularly useful option for understanding the effect of uncertainty and the application of SA techniques to uncertainty reduction problems is fast becoming an area of interest in current research efforts.

Sensitivity analysis approaches can be classified as either local or global. Local sensitivity analysis approaches determine the variation in the system outputs due to small uncertainty in the system inputs (Hamby 1994; Frey and Patil 2002; Kern et al. 2003), which might only be valid for small regions of uncertainty. On the contrary, global sensitivity analysis (Saltelli et al. 2008, GSA) accounts for the entire range of input uncertainty and determines its effect on the system outputs. The typical way that SA approaches are currently being used by designers is as methods for understanding the effects of system input uncertainty on system outputs (Iman and Helton 1988; Saltelli et al. 2000). The majority of the previous works in this particular application of SA have focused on systems where the uncertainty of input parameters has a presumed probabilistic distribution (e.g., Saltelli et al. 2000; Chen et al. 2005), or on systems where only one output at a time is considered (e.g., Sobol 2001; Helton and Davis 2003). Moreover, most of the current SA approaches are only applicable to single-disciplinary analysis-based engineering problems (Saltelli et al. 2000). In contrast to these single-disciplinary methods, SA approaches that treat multi-disciplinary systems in a more flexible multi-subsystem fashion are obviously more attractive as they can determine the sensitivity of subsystem's outputs more flexibly and capture the interaction effects between subsystems more accurately. Approaches addressing SA in a multi-disciplinary framework remain rare in the literature and all of them require probabilistic distributions for uncertainty (Gu et al. 1998; Yin and Chen 2008), or use gradient information of the function under consideration (Sobieszczanski-Sobieski 1990; Sobieszczanski-Sobieski et al. 1991; Noor et al. 2000). Moreover, in all the approaches currently in the literature, only one output is considered for each subsystem. However, almost all analysis models for engineering systems are multi-output in nature and probability distributions for uncertain inputs are not always known or valid (e.g., Rao and Cao 2002; Qiu et al. 2004; Wu and Rao 2007; Li and Azarm 2008).

A single-disciplinary uncertainty reduction method, called Multi-Objective Sensitivity Analysis (MOSA; Li 2007; Li et al. 2009), was recently developed using sensitivity analysis techniques. MOSA allows a designer to determine how much variation reduction in multiple outputs for an analysis model will result from an optimal reduction of input parameter uncertainty. Much like GSA methods, the MOSA approach can determine the sensitivity of output variations to multiple input parameter uncertainty, but limits this information to the combinations of parameter uncertainty which provide maximum output variation reduction at a minimal cost. This is done by using the associated costs of reducing parameter uncertainty (assuming those costs are known by the designer) to determine how much uncertainty need to be optimally reduced in each input parameter (or combination of parameters), given limited available resources. However, MOSA did not address the uncertainty reduction problem at each subsystem in a multi-disciplinary framework. Uncertainty in the input parameters of a multi-disciplinary engineering analysis system is not only unavoidable but also results in variations in the outputs at both the system and subsystem levels. Moreover, in a multi-disciplinary analysis model, uncertainty reduction in one parameter (or combination of parameters) may greatly improve the performance of one subsystem, but may have no effect, or perhaps even adverse effects on other coupled subsystems. For this reason, it is necessary that SA techniques be extended to multi-disciplinary problems with multiple outputs in order to consider the complex relationships between input uncertainty and outputs of the analysis in each subsystem and across coupled subsystems.

MIMOSA is capable of determining which subsystems are most sensitive to input uncertainty and then can determine how limited resources should be applied

to uncertainty reduction in order to obtain a maximum reduction in output variations at both the system and subsystem levels. The parameter uncertainty that MIMOSA is concerned with is assumed to be reducible and exists not only as input in each subsystem but also in the couplings between subsystems. However, MIMOSA does not require probability distribution information for uncertainty characterization, but instead assumes that an uncertain interval is known for each uncertain parameter. In the MIMOSA approach, given the known interval uncertainty for input parameters in both the system and subsystem levels, a designer can identify parameters whose uncertainty should be reduced or, perhaps even eliminated, in order to achieve the desirable reduction in variation in the system's and it's corresponding subsystem's outputs simultaneously. In additions, the relative importance of each of the subsystems can also be determined using the information produced by the MIMOSA approach. Two scalar metrics are used to quantify the amount of variation in outputs and the cost to the designer of reducing the uncertainty in the input parameters in both system and subsystem levels. A bi-objective SA problem is formulated in the system level problem and in each subsystem to minimize the variation in the corresponding system's outputs while simultaneously minimizing the investment required to produce the necessary reduction in the uncertainty of the system's parameters. A numerical example and an engineering design example, each having two or three subsystems, respectively, are used to demonstrate the applicability of the MIMOSA approach.

The rest of the paper is organized as follows. Some terminology and definitions used in the paper are described in Section 2. Details of the MIMOSA approach are presented in Section 3. Two examples, a numerical example having two subsystems and an engineering example having three subsystems, are presented in Section 4 to illustrate the applicability of the approach. Concluding remarks are presented in Section 5.

2 Definition and terminology

For completeness, several definitions and terms used throughout the paper are presented briefly next. The details of some of these definitions can also be found elsewhere (Li 2007; Li et al. 2009).

2.1 Tolerance region

A Tolerance Region (TR) for an analysis model of a design quantifies the amount of uncertainty associated with the model's input parameters. These are not selectable values, but are instead a property of a design under consideration that is known to possess uncertain input parameters. We presume that the uncertain input parameters have a nominal value $\boldsymbol{p}_0 = (p_0, 1, \ldots, p_{0,K})$ for $k = 1, \ldots, K$ uncertain parameters and a known interval (or range) of uncertainty, as shown in Fig. 1a for a two-parameter case. We describe the maximum parameter variation from the nominal in terms of input parameter variations $\Delta \boldsymbol{p} = (\Delta p_1, \ldots, \Delta p_K)$. Note that it is not necessary for the tolerance region to be symmetric about the nominal, or to be constant for all designs; however for simplicity in our work we have taken the TR to be symmetric, as this assumption makes the TR easier to visualize and simplifies the treatment of the TR in calculations involving this quantity. However, the additional complexity required to consider asymmetric tolerance regions would be trivial as discussed in Section 2.2 below. The uncertainty in parameters considered in this paper is assumed to be reducible. A parameter can be referred to as either a design variable (which defines a design) or any input to the analysis, such as material property, which is known to possess uncertainty.

2.2 Parameter uncertainty retention index and retained tolerance region

The vector $\alpha = (\alpha_1, \ldots, \alpha_K)$ is called the Parameter Uncertainty Retention Index (*PURI*) with $0 \leq \alpha_k \leq 1$, for $k = 1, \ldots, K$, one for each corresponding uncertain parameter.

A Retained Tolerance Region (RTR) is a region in the parameter space defined as the portion of an original TR, determined as the inner product of the *PURI* vector and the original TR: $\boldsymbol{\alpha}\, \Delta \boldsymbol{p} = (\alpha_1 \Delta p_1, \alpha_2 \Delta p_2, \ldots, \alpha_K \Delta p_K)$. Essentially, RTR can be any symmetric hyper-rectangle that is inside the original tolerance region centered at the nominal parameter value. When $\boldsymbol{\alpha} = \mathbf{1}$, the RTR is the original tolerance region and when $\boldsymbol{\alpha} = \mathbf{0}$, the RTR is reduced to the nominal value of the parameter, $\boldsymbol{p}_0$. For instance, in the two-dimensional case in Fig. 1b, $\alpha\, \Delta \boldsymbol{p}$ can represent any rectangle within the outer rectangle, depending on the selected value of *PURI*. If the uncertainty in a parameter is irreducible or only a portion of it is reducible, the corresponding lower bound for the elements in α can be set to be 1 or any specific value. For instance, if uncertainty in p_1 is completely irreducible then α_1 will always be equal to 1; while if the uncertainty in p_1 can only be reduced by 50%, then α_1 is limited to a minimum value of 0.5. In the case of an asymmetric TR about the nominal, additional K elements should

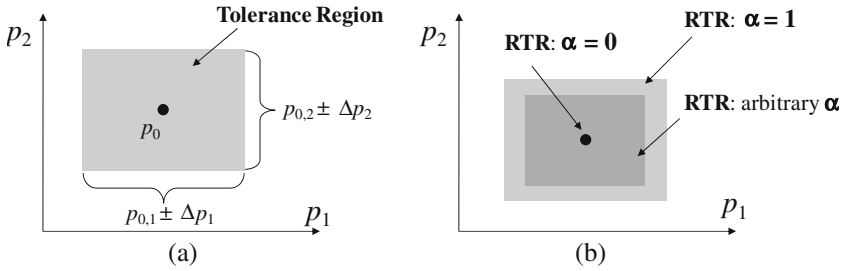

Fig. 1 **a** Tolerance region and **b** retained tolerance region

be added to the *PURI* vector and the size of the RTR would then be controlled by $2K$ elements; which is a trivial extension of the approach presented later in this paper.

Note that the *PURI* vector is a measure of the prescribed level of uncertainty reduction for the given uncertain parameters and is treated as a set of the decision variables in this paper. In other words, the *PURI* vector values will be selected within the MIMOSA algorithm, not by the designer beforehand.

2.3 Reduced output sensitivity region and acceptable output variation region

Regardless of which type of uncertainty (irreducible or reducible) is considered, it is possible to map the effects of input parameter variation for one or more designs under consideration into the output space and then evaluate those effects on the resulting uncertainty, in a multi-output sense. Given a known TR, which is characteristic of a given design and its associated uncertain parameters, (the left side of Fig. 2), the result of mapping that input uncertainty to the output space forms an Output Sensitivity Region (OSR; the right side of Fig. 2) for each design under consideration. Figure 2 assumes a two-input, two-output analysis model for several trial designs in the interest of visualization, but the concept is applicable to a problem of any size.

For a trial design $\boldsymbol{x}_0$, the nominal values of the M analysis outputs are $\boldsymbol{o}(\boldsymbol{x}_0, \boldsymbol{p}_0) = (o_1(\boldsymbol{x}_0, \boldsymbol{p}_0), \ldots, o_M(\boldsymbol{x}_0, \boldsymbol{p}_0))$. We will consider output variations of $\boldsymbol{x}_0$ caused by retained parameter variations $\boldsymbol{\alpha} \cdot \Delta \boldsymbol{p}$ as in (1):

$$\begin{aligned} &\Delta \boldsymbol{o}(\boldsymbol{x}_0, \boldsymbol{p}) = \boldsymbol{o}(\boldsymbol{x}_0, \boldsymbol{p}) - \boldsymbol{o}(\boldsymbol{x}_0, \boldsymbol{p}_0) \\ &\text{where} \quad \boldsymbol{p}_0 - \boldsymbol{\alpha}\, \Delta \boldsymbol{p} \le \boldsymbol{p} \le \boldsymbol{p}_0 + \boldsymbol{\alpha}\, \Delta \end{aligned} \tag{1}$$

Notice that the TR of parameters on the left of Fig. 2 can lead to different OSRs for the designs represented in the output space on the right of Fig. 2. This mapping of uncertain parameters into the output space can be quantified in the output space by measuring the distance of the largest deviation from the nominal point under the uncertain parameter intervals using an L_∞ norm. This quantification is denoted by R, or the Reduced OSR (ROSR) for $\boldsymbol{x}_0$, the design under consideration for analysis, as shown in (2):

$$\begin{aligned} &R(\boldsymbol{\alpha}) = \max_{\boldsymbol{p}} \left\| \frac{\Delta \boldsymbol{o}(\boldsymbol{p})}{\Delta \boldsymbol{o}_0} \right\| \\ &\text{where} \quad \begin{aligned} &\Delta \boldsymbol{o}(\boldsymbol{p}) = \boldsymbol{o}(\boldsymbol{x}_0, \boldsymbol{p}) - \boldsymbol{o}(\boldsymbol{x}_0, \boldsymbol{p}_0) \\ &\boldsymbol{p}_0 - \boldsymbol{\alpha}\ \Delta \boldsymbol{p} \le \boldsymbol{p} \le \boldsymbol{p}_0 + \boldsymbol{\alpha} \cdot \Delta \boldsymbol{p} \end{aligned} \end{aligned} \tag{2}$$

In (2), $\Delta \boldsymbol{o}_0$ is the Acceptable Output Variation Region (AOVR) for the M outputs. The AOVR value is specified by the designer and then the variation in those outputs is normalized by the corresponding AOVR values. The value of the AOVR is usually assumed by the designer who has good knowledge about the system or a clear requirement on the acceptable variation range of the system performance. Given an AOVR,

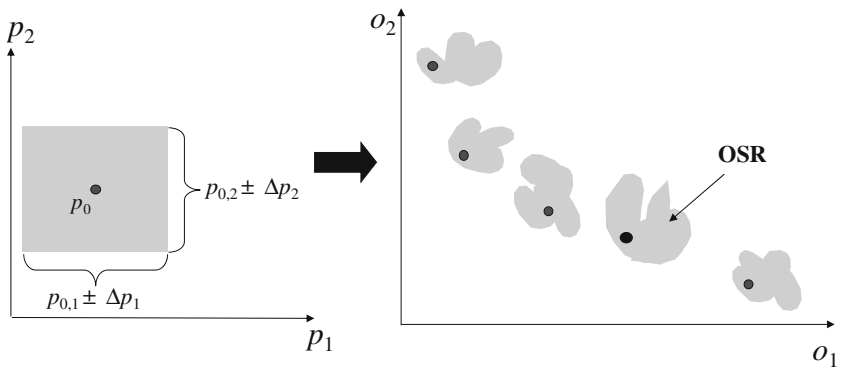

Fig. 2 Mapping from the tolerance region to the OSR

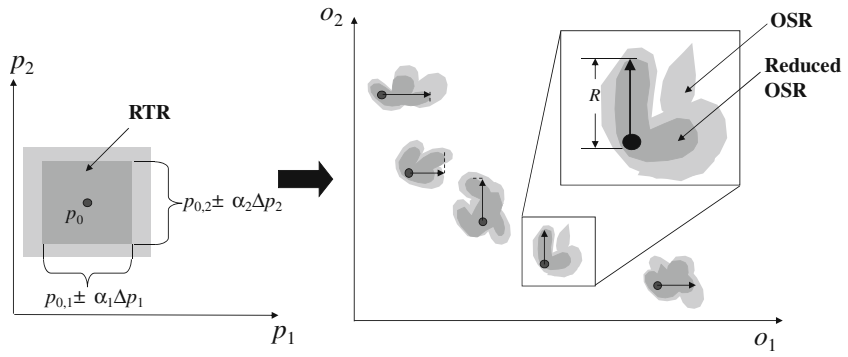

Fig. 3 Mapping from RTR to reduced OSR (ROSR) with variation R

it is required that the variation in the outputs to be less than the AOVR. As a result, R should be less than or equal to 1 for the acceptable variation for the outputs obtained from the analysis of a design $\boldsymbol{x}_0$. If an AOVR is not available or not desired, R can still be normalized instead by using the nominal output values. Normalization in (2) is usually necessarydepending on the applications, especially for the engineering analysis problems that have multiple outputs with different units or orders of magnitude.

As shown in Fig. 3, a measure of output variation R can be reduced (for multiple designs, as shown) by reducing the RTR for a given set of input parameters as R is a function of the corresponding *PURI* vector values for the system (or subsystem) of interest.

2.4 Correlation coefficient matrix

CC is a matrix of correlation coefficients calculated for a matrix whose rows are observed data of variables under consideration and whose columns are the variables. The (i, j)-th element of the matrix *CC* is defined as shown in (3), where $C(i, j)$ is the covariance value between variable i and variable j.

$$CC\,(i,\ j) = \frac{C\,(i,\ j)}{\sqrt{C\,(i,\ i)\,C\,(j,\ j)}} \tag{3}$$

2.5 Investment

As a measure of defining the cost of reducing uncertainty in input parameters, the concept of *Investment* is developed. The *Investment* metric, presented below, is essentially a notional function that correlates the amount of uncertainty to the "cost" required to produce that uncertainty reduction, and can be used in the absence of actual cost data or functions for an engineering analysis model. It can be easily extended to a metric for quantifying the real cost of uncertainty reduction by using a function or set of functions that accurately quantify the cost of reducing the specific uncertainties in each parameter of interest for a specific problem. For this paper, *Investment* is simply defined as the normalized representation of how much in terms of both perimeter and area (or volume) the uncertainty (or TR) of a set of parameters is reduced as a function of the *PURI* vector values, as detailed in (4):

$$Investment = \theta_1 \left(\frac{K - \sum_i^K \alpha_k}{K} \right) + \theta_2 \left(1 - \prod_i^K \alpha_k \right), \quad i = 1, \ldots, K \tag{4}$$

In (4) the quantities $\sum\alpha_k$ and $\prod\alpha_k$, respectively, represent the hyper-perimeter and hyper-volume of the uncertainty retained in the parameter space after the uncertainty is normalized by $\Delta\boldsymbol{p}$. The θ value can be selected and aligned according to the designer's preferences on the hyper-perimeter or the hyper-volume. In the work presented in this paper it is assumed that $\theta_1 = \theta_2 = 0.5$, meaning that both the volume and perimeter metrics have equal weights for reduction. The hyper-perimeter included in (4) indicates that the investment used to reduce uncertainty is linear to the amount of uncertainty in each parameter and identical for all parameters unless a weighting scheme is employed. Additionally, the hyper-volume included in (4) describes that the investment is proportional to the product of uncertainty reduction for all parameters, which accounts for the total volume of uncertainty reduction given a set of *PURI* values. It can be seen from (4) that as the *PURI* vector elements go to 0, *Investment* goes to 1 indicating that a maximum possible effort is required to eliminate all the uncertainty in the input parameters, while as all α_k values go to 1, *Investment* tends to 0 meaning no resources are required to reduce the input uncertainty. Clearly *Investment* and R are competing metrics as smaller output variation levels will always require greater cost. It should be noted that if any

real utility or cost function associated with parameter uncertainty reductions is available for specific applications, such as a known dollar value required per unit of machining tolerance improvement for a geometric dimension, it can be easily incorporated into (4).

2.6 Multi-disciplinary multi-output analysis system

Equation (5) and Fig. 4 depict a typical multi-disciplinary multi-output system where a multi-disciplinary system is decomposed into three coupled subsystems that share some design variables and input parameters, respectively represented as $\boldsymbol{x}_{sh}$ and $\boldsymbol{p}_{sh}$, along with their local subsystem variables and parameters $\boldsymbol{x}_i$ and $\boldsymbol{p}_i$, i= 1, 2, 3. The subsystem's outputs can be single or multiple and are used to resolve the system level outputs. In (5), $\boldsymbol{y}_{ij}$ represents a coupling variable vector: Outputs from subsystem i (SSi) and inputs to subsystem j (SSj). The vector $\boldsymbol{x}_i$ and $\boldsymbol{o}_i$ are SSi's design variables and outputs, respectively. The vector $\boldsymbol{Y}_i$ in (5) represents the functions that are used to calculate the coupling variables $\boldsymbol{y}_{ij}$. Parameters $\boldsymbol{p}_i$ represent the local uncertain parameters that have interval uncertainty. The entire system outputs can be represented by the vector $\boldsymbol{o}_0$, which can be assumed to be functions of shared design variables, parameters, and local (subsystem) outputs, respectively.

Given the shared and local design variables $\boldsymbol{x}_{sh}$ and $\boldsymbol{x}_i$, which specify the candidate design(s), the variations in the system and subsystem outputs are dependent on the uncertain input parameters and coupling variables.

$$\begin{aligned} &\boldsymbol{o}_i = \boldsymbol{O}\left(\boldsymbol{x}_{sh}, \boldsymbol{p}_{sh}, \boldsymbol{x}_i, \boldsymbol{p}_i, \boldsymbol{y}_{ji}\right) \\ &\text{where} \quad \boldsymbol{y}_{ij} = \boldsymbol{Y}_i\left(\boldsymbol{x}_{sh}, \boldsymbol{p}_{sh}, \boldsymbol{x}_i, \boldsymbol{p}_i, \boldsymbol{y}_{ji}\right) \quad i = 1, 2, 3 \end{aligned} \tag{5}$$

One typical method to hierarchically decouple a fully (two-way) coupled multi-output multi-disciplinary system is to introduce a new set of variables at the system level, indicated in Fig. 5 as $\boldsymbol{t}$, which represent target values, one for each of the coupling variables that connect the subsystems, (e.g., Aute and Azarm 2006). Each subsystem (SSi) uses the target variables to perform local calculations to obtain all local output values (i.e., $\boldsymbol{o}_i$,and $\boldsymbol{y}_{ij}$). The collaborative consistency of the system is maintained by enforcing a consistency constraint in each subsystem. This consistency constraint requires that the value of each element of $\boldsymbol{y}_{ij}$ converges to its corresponding target value in $\boldsymbol{t}_{ij}$ in the deterministic case. These new variables, $\boldsymbol{t}$, are considered as design variables to be given along with the shared design variables $\boldsymbol{x}_{sh}$, at the system level (SS0).

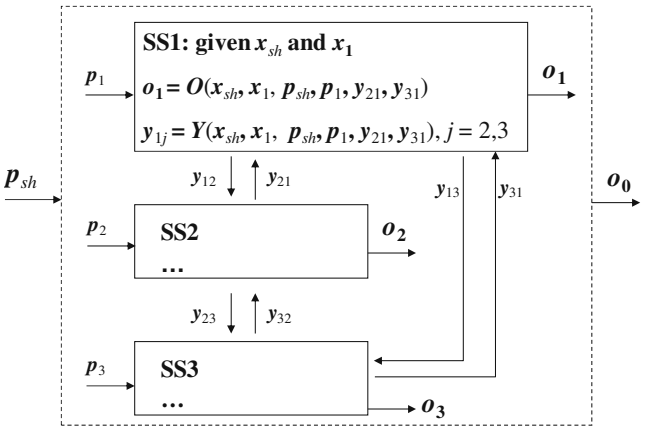

Fig. 4 A multi-disciplinary system with three subsystems

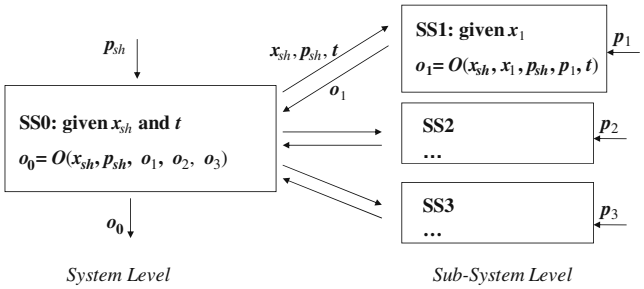

Fig. 5 Multi-output multi-disciplinary system in a two-level decomposed framework

3 MIMOSA

In this section the specifics of the MIMOSA approach are presented. The issue as to how to ensure the collaborative consistency of a multi-disciplinary system under uncertainty is addressed in Section 3.1. The formulation of the MIMOSA approach is outlined in Section 3.2. The detailed steps of MIMOSA are presented in Section 3.3.

3.1 Collaborative consistency of MIMOSA

As mentioned previously, in order to decouple the multiple subsystems that make up a multi-disciplinary system and maintain the collaborative consistency of the system, a target variable for each coupling variable must be introduced at the system level and then used in each subsystem. However, when uncertainty is considered in the system the collaborative consistency of the system is not straightforward and deserves more attention (Li and Azarm 2008). A multi-disciplinary system is said to possess collaborative consistency when all subsystems achieve the same value for each coupling variable within the system's decomposed framework,

thus ensuring that subsystems will work together consistently to analyze a design.

When considering the subsystem couplings shown in Fig. 4, the propagation of uncertainty implies that outputs from one subsystem are not only affected by the uncertainty from this subsystem's parameters but also by the uncertainty in coupling variables. With the introduction of interval uncertainty in parameters, the collaborative consistency constraint can no longer be satisfied since the uncertainty in the input parameters $\boldsymbol{p}_i$ of SSi leads to a range rather than a single value for each component in the coupling variables $\boldsymbol{y}_{ij}$. The collaborative consistency constraint in SSi cannot force a range of output values for each coupling variable $\boldsymbol{y}_{ij}$ to converge to a single target value of $\boldsymbol{t}_{ij}$. As a result, a system and corresponding subsystems could become inconsistent due to a mismatch between the output range of each coupling variable and the deterministic value of each target variable. To resolve this mismatch the target variables $\boldsymbol{t}$ must be able to tolerate the resulting variation ranges in the coupling variables $\boldsymbol{y}$. In other words, to accept the variation in the coupling variables $\boldsymbol{y}$, target variables $\boldsymbol{t}$ should have an associated tolerance range. Given a candidate design, as long as the established tolerance range of $\boldsymbol{t}_{ij}$ encloses the resultant variation in $\boldsymbol{y}_{ij}$ for the system, the variations in coupling variables $\boldsymbol{y}_{ij}$ can be absorbed by a local TR of the targets $\boldsymbol{t}_{ij}$ for SSj, ensuring that the system will remain collaboratively consistent.

To accommodate the propagation of uncertainty, it is necessary to ensure that the selected tolerance regions associated with the target variables are large enough to enclose the expected variations in the corresponding coupling variables in order to maintain the feasibility of the entire system. This tension between uncertainty reduction and collaborative consistency is resolved in the MIMOSA approach by adding a new collaborative consistency constraint under uncertainty in each subsystem. In order for this new constraint to function properly and have the desired result of ensuring the overall system consistency, all target variables which are a part of the collaborative consistency constraints are considered to have interval uncertainty at the system level and have corresponding *PURI* vector values selected to control the associated uncertainty. Using this method, as long as the resultant variation in the coupling variables output from each subsystem is less than the retained uncertainty in the target variables passed down from the system level, the collaborative consistency among subsystems will be ensured (see the next subsection for a detailed formulation). The selection on the original TR of the target variabls are dependend on the designer's opinion or specific requirments on couplings.

3.2 Formulation of MIMOSA

For simplicity, the formulation of the MIMOSA approach will be presented as applied to a single candidate design, but extending this approach to multiple candidate designs is straightforward to accomplish (see Li et al. 2009). The MIMOSA approach, as shown in Fig. 6, consists of performing a two-objective optimization problem for SA at the system level and for each subsystem in a decomposed framework. The SA optimization problem is used to determine the best R and

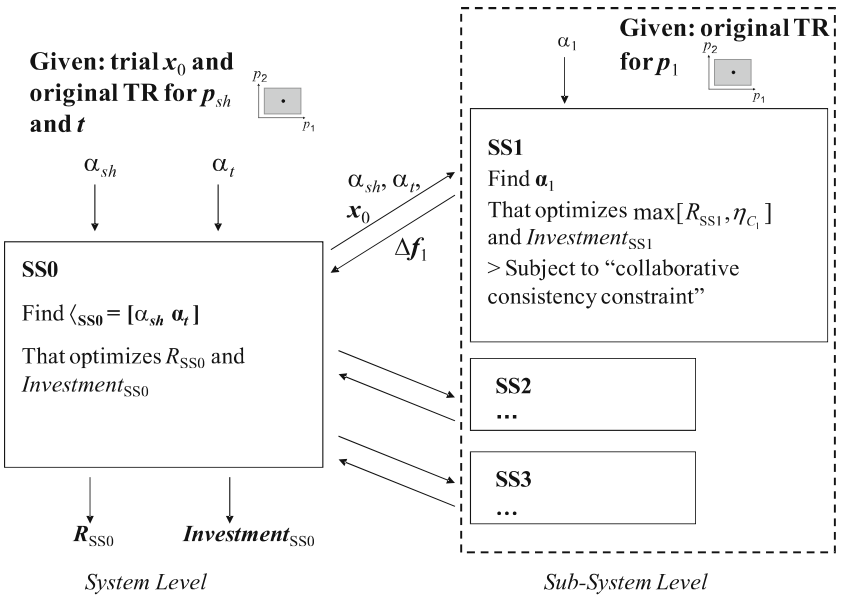

Fig. 6 MIMOSA formulation

Investment attainable as a function of the *PURI* vector for uncertain parameters $\boldsymbol{p}$ and the target variables $\boldsymbol{t}$. This is conducted at the system level and in each of the subsystems being considered in a bi-level fashion. The formulation assumes that the designer already has obtained a candidate design (or designs) in which input parameters have reducible interval uncertainty.

At the system level (SS0), the variables are the *PURI* vector $\boldsymbol{\alpha}_{\mathrm{SS0}}$, which includes $\boldsymbol{\alpha}_{sh}$ and $\boldsymbol{\alpha}_t$ for $\boldsymbol{p}_{sh}$ and $\boldsymbol{t}$, respectively. The two objectives of the SA optimization at the system level are (1) to minimize *Investment* and (2) to minimize the variation in the system level design outputs represented as R_{SS0}, as shown in (6). Here, R_{SS0} at the system level is defined as the L_∞ norm of the variation in the corresponding system outputs.

$$\begin{aligned} &\min_{\boldsymbol{\alpha}_{\mathrm{SS0}}} R_{\mathrm{SS0}} = \|\Delta \boldsymbol{o}_{\mathrm{SS0}}\|_\infty \\ &\min_{\boldsymbol{\alpha}_{\mathrm{SS0}}} \mathit{Investment}_{\mathrm{SS0}} \end{aligned} \tag{6}$$

where

$$\begin{aligned} &\Delta \boldsymbol{o}_{\mathrm{SS0}} = \boldsymbol{o}_0(\boldsymbol{x}_0, \boldsymbol{p}) - \boldsymbol{o}_0(\boldsymbol{x}_0, \boldsymbol{p}_0) \\ &\boldsymbol{p}_0 - \boldsymbol{\alpha}_{\mathrm{SS0}} \cdot \Delta \boldsymbol{p} \le \boldsymbol{p} \le \boldsymbol{p}_0 + \boldsymbol{\alpha}_{\mathrm{SS0}} \cdot \Delta \boldsymbol{p} \\ &\boldsymbol{\alpha}_{\mathrm{SS0}} \equiv [\boldsymbol{\alpha}_{sh}, \boldsymbol{\alpha}_t] \end{aligned}$$

In (6), $\Delta \boldsymbol{o}_{\mathrm{SS0}}$ is the variation in SS0's outputs. If the outputs in SS0 have different units or different orders of magnitude with respect to each other, the normalization of the variation in the system level's (SS0) outputs is necessary. The most obvious choice is to normalize $\Delta \boldsymbol{o}_{\mathrm{SS0}}$ by the nominal output values for a candidate design under consideration.

The formulation of the subsystem SA problem is very similar to the system level, with the key addition of the need to ensure collaborative consistency of the design under uncertainty. To do this consistency check under uncertainty, in each subsystem level optimization problem, SSi, the quantity η_C is defined as the maximum $||\cdot||_\infty$ distance from the coupling variable $\boldsymbol{y}_{ij}$ to the nominal target variable $\boldsymbol{t}_{ij,0}$, as shown in (7a). As long as this distance is within the optimizer-specified retained tolerance region $\boldsymbol{\alpha} \cdot \Delta \boldsymbol{t}_{ij,0}$for target variables, the variation in the coupling variable is acceptable.

$$\eta_{C_i} = \max_{\boldsymbol{p},\, t} \|C_i\|_\infty, \; i = 1,\; 2,\; 3 \tag{7a}$$

Equation (7b) below details the value C_i, used in (7a), which quantifies the difference between $\boldsymbol{y}_{ij}$ and the nominal value of $\boldsymbol{t}_{ij}$, normalized by the RTR of $\boldsymbol{t}_{ij}$. Recall that $\boldsymbol{\alpha} \cdot \Delta \boldsymbol{t}_{ij}$ is the retained tolerance region for target variables $\boldsymbol{t}_{ij}$, in which $\boldsymbol{\alpha}$ is determined by the system level optimizer and sent to SSi from SS0:

$$\begin{aligned} &C_i = \tfrac{y_{ij}(\boldsymbol{x},\, \boldsymbol{p},\, \boldsymbol{t}_{ji}) - \boldsymbol{t}_{ij,0}}{\boldsymbol{\alpha} \,\Delta\, \boldsymbol{t}_{ij}}, \;\; j \ne i \\ &\boldsymbol{p}_0 - \boldsymbol{\alpha}\, \Delta \boldsymbol{p} \le \boldsymbol{p} \le \boldsymbol{p}_0 + \boldsymbol{\alpha}\, \Delta \boldsymbol{p} \\ &\boldsymbol{t}_{ji,0} - \boldsymbol{\alpha}\, \Delta \boldsymbol{t}_{ji} \le \boldsymbol{t}_{ji} \le \boldsymbol{t}_{ji,0} + \boldsymbol{\alpha} \,\Delta\, \boldsymbol{t}_{ji} \\ &\boldsymbol{p} \equiv \left[\boldsymbol{p}_{sh}, \boldsymbol{p}_i\right], \;\; \boldsymbol{\alpha} \equiv [\boldsymbol{\alpha}_{\mathrm{SS0}}, \boldsymbol{\alpha}_i] \end{aligned} \tag{7b}$$

For the SA problem in subsystem i (SSi), the decision variables are the*PURI* vector $\boldsymbol{\alpha}_i$ for the local uncertainty parameters $\boldsymbol{p}_i$. The two objectives for each subsystem are again to minimize $\mathrm{Investment}_{\mathrm{SS}i}$ while simultaneously minimizing the maximum of either the output variation at the local subsystem level $R_{\mathrm{SS}i}$, or the variation in coupling variables, η_{Ci} in SSi. In (8), $R_{\mathrm{SS}i}$is again a measure of the variation in the subsystem's outputs, here normalized by the corresponding subsystem's AOVR $\Delta \boldsymbol{o}_{0,i}$, which is the presumed acceptable variation for the subsystem's outputs. This optimization problem is subject to two constraints as shown in (8), including: (1) the variation in the SSi's original outputs must be enclosed by the designated AOVR of SSi; and (2) the variation in coupling variables must be less than the retained tolerance region of target variables (determined in SS0). These constraints must be satisfied in all subsystems in order to maintain the consistency of the system under uncertainty. Thus the SA optimization problem formulation in SSi is as follows:

$$\begin{aligned} &\min_{\alpha_i} \max\left[R_{\mathrm{SS}i}, \eta_{C_i}\right] \\ &\min_{\alpha_i} \mathit{Investment}_{\mathrm{SS}i} \\ &s.t. \\ &\quad \max\left[R_{\mathrm{SS}i}, \eta_{C_i}\right] \le 1 \\ &\quad R_{\mathrm{SS}i} = \max_{\boldsymbol{p}, \boldsymbol{t}_{ji}} \left\| \tfrac{\Delta \boldsymbol{o}_i(\boldsymbol{p})}{\Delta \boldsymbol{o}_{0,i}} \right\|_\infty, \; \eta_{C_i} = \max_{\boldsymbol{p}, \boldsymbol{t}_{ji}} \|C_i\|_\infty \end{aligned} \tag{8}$$

where $C_i = \tfrac{y_{ij}(\boldsymbol{x}_0, \boldsymbol{p}, \boldsymbol{t}_{ji}) - \boldsymbol{t}_{ij,0}}{\boldsymbol{\alpha} \cdot \Delta \boldsymbol{t}_{ij}}, \; j \ne i$

$$\begin{aligned} &\Delta \boldsymbol{o}_i(\boldsymbol{p}) = \boldsymbol{o}_i(\boldsymbol{x}_0, \boldsymbol{p}) - \boldsymbol{o}_i(\boldsymbol{x}_0, \boldsymbol{p}_0) \\ &\boldsymbol{p}_0 - \boldsymbol{\alpha} \cdot \Delta \boldsymbol{p} \le \boldsymbol{p} \le \boldsymbol{p}_0 + \boldsymbol{\alpha} \cdot \Delta \boldsymbol{p} \\ &\boldsymbol{t}_{ji,0} - \boldsymbol{\alpha} \cdot \Delta \boldsymbol{t}_{ji} \le \boldsymbol{t}_{ji} \le \boldsymbol{t}_{ji,0} + \boldsymbol{\alpha} \cdot \Delta \boldsymbol{t}_{ji} \\ &\boldsymbol{p} \equiv \left[\boldsymbol{p}_{sh}, \boldsymbol{p}_i\right], \boldsymbol{\alpha} \equiv [\boldsymbol{\alpha}_{\mathrm{SS0}}, \boldsymbol{\alpha}_i] \end{aligned}$$

The MIMOSA formulation is also shown in Fig. 6 at both system and subsystem levels.

A simplified formulation of MIMOSA at the subsystem level is also provided as shown in (9), for the cases where a designer does not know or specify an AOVR for the subsystem outputs. In this regard, as long as the overall system is collaboratively consistent by enforcing the constraint on η_{Ci} in (9), the solution found will be acceptable. In this simplified formulation, normalization of $R_{\mathrm{SS}i}$ is still necessary in order to handle the

possibility of different units or orders of magnitude in the subsystem outputs, and is accomplished by using the nominal output values. However, the value of R_{SSi} is usually much less than the value of η_{Ci} in this formulation and as a result the first objective of the SA problem for each subsystem should only minimize R_{SSi} alone.

$$\begin{aligned} &\min_{\alpha_i} \ R_{SSi} \\ &\min_{\alpha_i} \ Investment_{SSi} \\ &s.t. \\ &\quad \eta_{C_i} \le 1 \\ &\quad R_{SSi} = \max_{\boldsymbol{p},\boldsymbol{t}_{ji}} \left\| \frac{\Delta \boldsymbol{o}_i(\boldsymbol{p})}{\boldsymbol{o}_i(\boldsymbol{x}_0,\boldsymbol{p}_0)} \right\|_\infty, \quad \eta_{C_i} = \max_{\boldsymbol{p},\boldsymbol{t}_{ji}} \|C_i\|_\infty \end{aligned} \tag{9}$$

where $C_i = \frac{y_{ij}(\boldsymbol{x}_0,\boldsymbol{p},\boldsymbol{t}_{ji}) - \boldsymbol{t}_{ij,0}}{\boldsymbol{\alpha}\cdot\Delta\boldsymbol{t}_{ij}}$, $j \neq i$

$$\begin{aligned} &\Delta \boldsymbol{o}_i(\boldsymbol{p}) = \boldsymbol{o}_i(\boldsymbol{x}_0, \boldsymbol{p}) - \boldsymbol{o}_i(\boldsymbol{x}_0, \boldsymbol{p}_0) \\ &\boldsymbol{p}_0 - \boldsymbol{\alpha}\cdot\Delta\boldsymbol{p} \le \boldsymbol{p} \le \boldsymbol{p}_0 + \boldsymbol{\alpha}\cdot\Delta\boldsymbol{p} \\ &\boldsymbol{t}_{ji,0} - \boldsymbol{\alpha}\cdot\Delta\boldsymbol{t}_{ji} \le \boldsymbol{t}_{ji} \le \boldsymbol{t}_{ji,0} + \boldsymbol{\alpha}\cdot\Delta\boldsymbol{t}_{ji} \\ &\boldsymbol{p} \equiv [\boldsymbol{p}_{sh}, \boldsymbol{p}_i], \ \boldsymbol{\alpha} \equiv [\boldsymbol{\alpha}_{SS0}, \boldsymbol{\alpha}_i] \end{aligned}$$

In Section 4, (8) and (9) will be used in the numerical and engineering example, respectively.

Notice first that in (6) for SS0 and (8) (or (9)) for SS*i*, we do not require any additional information on the input-output relation from the analysis models. The analysis models in SS0 and SS*i* are treated like black-boxes and can be any kind of functions or computer simulations as long as the input and output values are provided. In addition, if we intentionally fix one α value in the *PURI* vector to be zero and all other elements to be one, we can essentially "leave one [parameter] out" and calculate the corresponding R_{SSi} value. By repeating this for each parameter (or combination of parameters), the quantitative comparison on the importance of the parameter(s) can be obtained as using a traditional "leave one out" GSA method. However, the MIMOSA approach is more capable in that it allows every α value not only to be zero or one but also any value between them, optimally determined by the optimizer. In this regard, all uncertain input parameters in one subsystem can vary within the RTR specified by the *PURI* vector and can affect the variation in subsystem outputs simultaneously. Thus, not only the main effect of each parameter, but also the interaction effects of those parameters are considered in this approach, within the optimal uncertainty ranges. The individual importance of each parameter can also be determined from the resulting optimal solutions to (6) and (8) as discussed later in Section 4. Due to the system properties considered by the MIMOSA approach, e.g., multi-input, multi-output, black-box analysis models, and most importantly, variable uncertainty ranges (i.e., not just zero or one for $\boldsymbol{\alpha}$ values), the MIMOSA approach is capable of providing more information about a system than produced by the other existing multi-disciplinary GSA approaches reviewed in Section 1.

3.3 Steps of MIMOSA

In order to perform the MIMOSA approach described above, an algorithm is developed and a step-by-step description of that algorithm follows. All system and subsystem SA problem optimizations are accomplished using evolutionary algorithms or more specifically using the Multi-Objective Genetic Algorithm (MOGA; Deb 2001). The usage of MOGA to solve the system or sub-system level problems is not required and other multi-objective optimization approaches could also be applied, if applicable and desired. However, MOGA is used in this paper because of its flexibility in finding all Pareto solutions simultaneously, its ability to handle non-linear and non-differentiable output functions with both continuous and/or discrete variables, and its ease in incorporating "black-box" type simulations. These properties are very common in the real engineering applications that are the target problems of this approach. However, MOGA is not the only choice of optimization solvers for use in this approach. The decomposed SA optimization formulation is solved using a multi-objective multi-disciplinary optimization technique (Aute and Azarm 2006). The MIMOSA steps are as follows:

Step 1. Select a candidate design alternative (or a trial design), $\boldsymbol{x}_0$, whose sensitivity analysis is to be studied.

Step 2. Select which input parameters are to be studied, and then determine the interval uncertainty for those parameters, specifying the original TR, $\boldsymbol{p} = [\boldsymbol{p}_0 + \Delta\boldsymbol{p}, \ \boldsymbol{p}_0 - \Delta\boldsymbol{p}]$ for all parameters at the system and subsystem levels.

Step 3. Select the original TR for target values $\boldsymbol{t} = [\boldsymbol{t}_0 + \Delta\boldsymbol{t}, \ \boldsymbol{t}_0 - \Delta\boldsymbol{t}]$ at the system level.

Step 4. Initialize the optimization problem at the system level (SS0) as in (6), given the system level design $\boldsymbol{x}_{sh}$ and original TR for $\boldsymbol{p}_{sh}$, and $\boldsymbol{t}$.

Step 5. Select the initial value for *PURI*, $\boldsymbol{\alpha}_{SS0}$, at the system level for each element in $\boldsymbol{p}_{sh}$ and $\boldsymbol{t}$, and use $\boldsymbol{\alpha}_{SS0}$ to calculate Investment_{SS0}.

Step 6. Send the system design variables, nominal shared parameters, nominal target values, and system level *PURI* $\boldsymbol{\alpha}_{SS0}$ to each subsystem level SA problem.

Step 7. Simultaneously initialize the SA approach in each subsystem level problem (SS*i*), given the $\boldsymbol{x}_{sh}$, $\boldsymbol{\alpha}_{SS0}$, $\boldsymbol{p}_{sh}$, and $\boldsymbol{t}$ values from SS0 along with subsystem variables and parameters, including initial *PURI* $\boldsymbol{\alpha}_i$ for the subsystem level uncertain parameters.

Step 8. Determine the optimal $\boldsymbol{\alpha}_i$ to the optimization problem in (8) or (9) for each subsystem using MOGA, considering the variation in subsystem's outputs (i.e., the variation in outputs and/or coupling variables) and *Investment* as the objectives, while ensuring the collaborative consistency constraint and/or AOVR constraint.

Step 9. Return optimal output values and local optimal *PURI* vector $\boldsymbol{\alpha}_i$ to the system level (SS0) from the subsystems. If more than one local optimal solution $\boldsymbol{\alpha}_i$ is identified, some selection strategy should be used to select one local optimal solution for each subsystem. In this paper, two selection strategies have been used: the optimal solution from the SS*i*'s Pareto with the maximum and minimum R_{SSi} value will be selected as the subsystem's single optimal solution in the numerical example and the engineering example in Section 4, respectively, and will be returned back to SS0. Other appropriate strategies for selecting a single solution from the subsystem Pareto are also acceptable.

Step 10. Analyze system level *R* vs. *Investment* Pareto optimal solutions to (6) for *PURI* vector, $\boldsymbol{\alpha}_{SS0}$.

Step 11. Check stopping criteria of the system level SA problem. If stopping criteria are satisfied, stop the algorithm; otherwise generate a new set of candidates of *PURI* vector $\boldsymbol{\alpha}_{SS0}$ at the system level from the optimizer, go to *Step 5*, and repeat subsystem level optimizations.

The stopping criteria used is a pre-specified maximum number of iterations (which is large enough to ensure convergence), plus an additional complementary stopping criterion that further requires that a sufficient number of Pareto solutions are produced during several successive generations. In other words, when the number of Pareto solutions is more than some pre-specified percentage of the population size and when it becomes steady (e.g., the number of Pareto solutions is more than "40% population size", for several generations), it can be concluded that the algorithm has converged. Compared to single-disciplinary SA approaches, the computational effort in this new MIMOSA approach will be larger due to the bi-level nature of the problem and will increase further when the number of subsystems considered is increased, since a SA optimization problem (as shown in (8)) must be solved for each subsystem considered. If the number of function calls in SS0 in (6) is N_{SS0} and the number of function calls in each subsystem is N_{SSi} and the number of function calls to evaluate R_{SSi} in each subsystem is N_R, then the total number of function calls in MIMOSA is $O\left[N_{SS0} \times NumSS\left(N_{SSi} \times N_R\right)\right]$, where NumSS is the number of subsystems. The computational cost of MIMOSA may increase when the number of subsystems and/or the number of system inputs are increased.

4 Examples and results

In this section, a numerical example and an engineering example are presented to demonstrate the applicability of the MIMOSA approach. Equations (8) and (9), as well as different selection strategies discussed above in Step 8 of Section 3.3, are used in those two examples, respectively, for the subsystem level SA problems.

4.1 Numerical example

A two-output, bi-level numerical example is adapted from a previously presented bi-level MDO problem with two coupled subsystems (Li and Azarm 2008). The two-output formulation for this problem in a single-disciplinary (or all-at-once) formulation is given in (10). There are three design variables: $\boldsymbol{x} = [x_1,\ x_2,\ x_3]$, two output functions: $\boldsymbol{o} = [o_1,\ o_2]$.

$$\begin{aligned} o_1 &= x_2^2 + x_3 + y_1 + e^{-y_2} \\ o_2 &= x_1 + \sqrt{x_2} + \left(y_2^2 - y_1^3\right)/10^4 + 150 \end{aligned} \tag{10}$$

The two coupling variables are y_1 and y_2 which make the two subsystems fully coupled:

$$\begin{aligned} y_1 &= \boldsymbol{Y}_1\left(\boldsymbol{x},\ y_2\right) = x_1^2 + x_2 - 0.2y_2 \\ Y_2 &= \boldsymbol{Y}_2\left(\boldsymbol{x},\ y_1\right) = x_1 + x_3 + \sqrt{y_1} \end{aligned} \tag{11}$$

The above all-at-once formulation is converted into a system level and two subsystem level SA problems. Between these two subsystems SS*i*, *i*= 1 and 2, there are two coupling variables $\boldsymbol{y} = \left[y_1,\ y_2\right]$. In each subproblem, there are two outputs in additional to the coupling variable. The decomposed formulation for this problem is as follows.

In SS0, $\boldsymbol{x}_{sh}$ includes only one design variable x_1 and the vector of target variables $\boldsymbol{t}$ includes two target variables t_1 and t_2, corresponding to the two coupling variable y_1 and y_2. Thus $\boldsymbol{x}_{sh} = [x_1]$, $\boldsymbol{t}_{12} = [t_1]$ and $\boldsymbol{t}_{21} -$

$[t_2]$. Each output in SS0 is the summation of the corresponding outputs of two subsystems as shown in (12), where $o_{i,j}$, i, j= 1 and 2, is jth output in SSi and calculated from (13) and (14) below:

$$\begin{aligned} o_{0,1} &= o_{1,1} + o_{2,1} = y_1 + x_2^2 + x_3 + e^{-y_2} \\ o_{0,2} &= o_{1,2} + o_{2,2} = -y_1^3/10^4 + 150 \\ &\quad + \sqrt{x_2} + y_2^2/10^4 + x_1 \end{aligned} \tag{12}$$

SS1 has the local design variable: $\boldsymbol{x}_1 = [x_2]$, and the local copy of the target variable for t_2, i.e., t_2^1. The two outputs of SS1 plus the coupling variable y_1 are given in (13):

$$\begin{aligned} o_{1,1} &= x_2^2 + y_1 \\ o_{1,2} &= \sqrt{x_2} - y_1^3/10^4 + 150 \\ y_1 &= x_1^2 + x_2 - 0.2t_2^1 \end{aligned} \tag{13}$$

Similarly, SS2 has the local design variable $\boldsymbol{x}_2 = [x_3]$ and the local copy of the target variable for t_1, i.e., t_1^2. The two outputs of SS2 plus the coupling variable y_2 are given in (14):

$$\begin{aligned} o_{2,1} &= x_3 + e^{-y_2} \\ o_{2,2} &= x_1 + y_2^2/10^4 \\ y_2 &= x_1 + x_3 + \sqrt{t_1^2} \end{aligned} \tag{14}$$

The interval uncertainty is assumed in input variables x_1, x_2 and x_3, within ±6% from nominal. The AOVR for the outputs $\boldsymbol{o}_1$ and $\boldsymbol{o}_2$ in SS1 and SS2 is ±5 units from their nominal. The original TR for the target variables is: $[\Delta t_1,\ \Delta t_2] = [\pm 4,\ \pm 3]$ units from their nominal. The candidate design alternative selected is $\boldsymbol{x}_0$: $[x_1, x_2, x_3, t_1, t_2] = [-5.478, 0.035, 0.410, 30.262, 0.448]$. The variables at the system level are $\boldsymbol{\alpha}_{SS0} \equiv [\alpha_{x1}, \alpha_{t1}, \alpha_{t2}]$. Here it is assume that not all of the uncertainties in the system can be completely reduced for each parameter, so α_{t1} and α_{t2} are assumed to be in the ranges [0.3, 1] and [0, 1], respectively. At the subsystem level, the design variable in SS1 and SS2 are

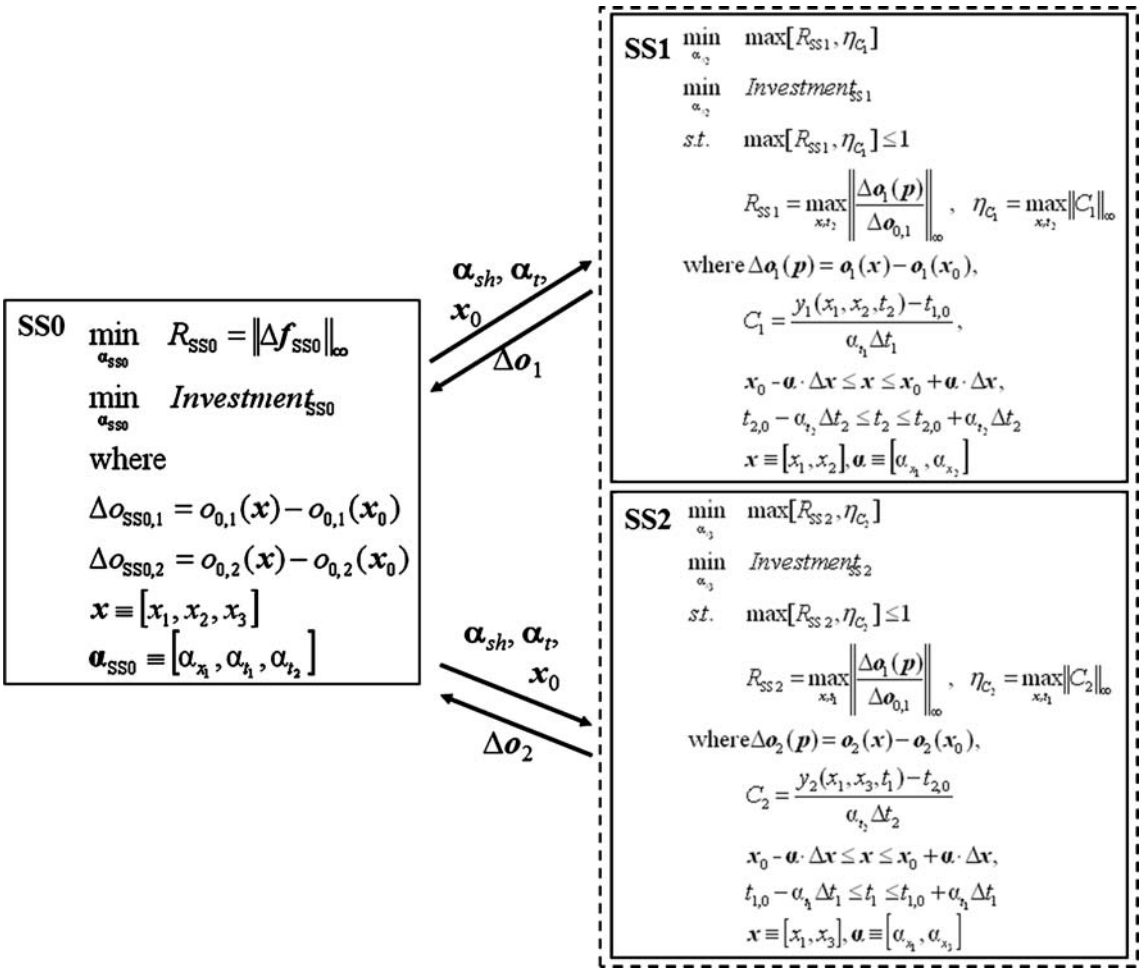

Fig. 7 Numerical example: the MIMOSA formulation

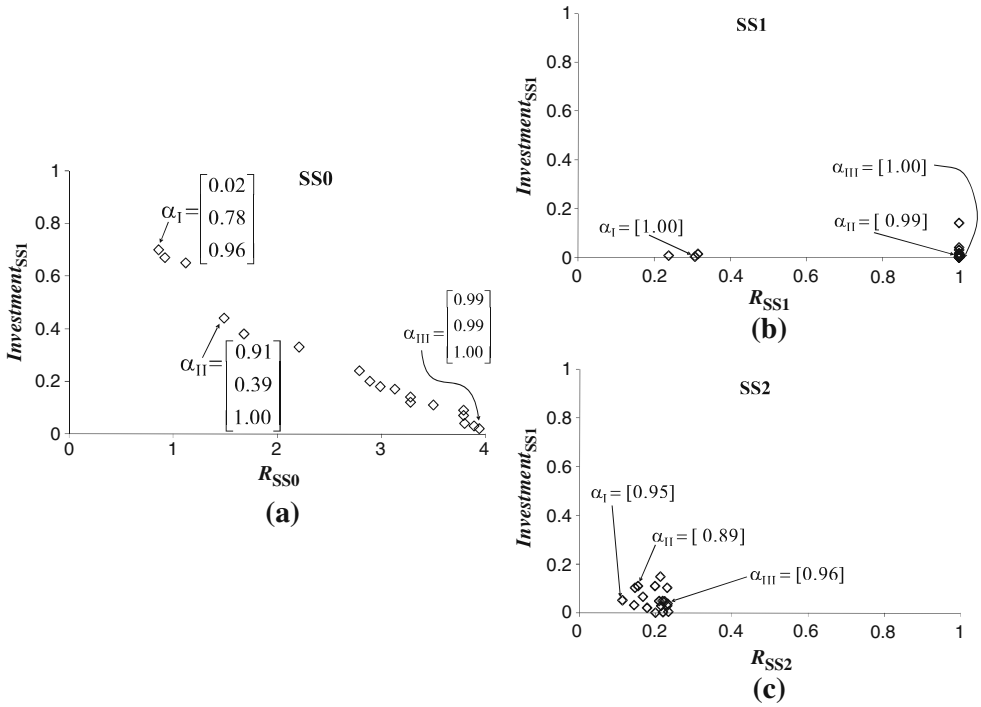

Fig. 8 Numerical example: Pareto solutions at **a** SS0, **b** SS1 and **c** SS2

$\boldsymbol{\alpha}_1 \equiv [\alpha_{x2}]$ and $\boldsymbol{\alpha}_2 \equiv [\alpha_{x3}]$ which are in the range [0, 1]. The MIMOSA formulation of this example for SS0, SS1 and SS2 is shown in Fig. 7. The Pareto solutions are shown in Fig. 8.

In this example, the optimal solution from the SS*i*'s Pareto with the maximum R_{SSi} value is selected as the subsystem's single optimal solution and is sent back to SS0. This selection strategy is used in the cases that the designers in the subsystems prefer the optimal α_i with the minimum investment as long as the AOVR and consistency constraints are satisfied.

The obtained Pareto solutions with three typical $\boldsymbol{\alpha}$ solutions at the system and subsystem levels using the formulation in (8) are shown in Fig. 8 as well as in Table 1. The trade-off between the *Investment* and variation in SS0's outputs, R_{SS0} are clear. R_{SS0} (the variation in SS0) is decreasing with the increasing of *Investment*. As shown in Table 1, $\boldsymbol{\alpha}_{III} = [0.99\ 0.99\ 1]$ gives almost the original TR, which represents the maximum uncertainty in the input parameters. $R_{SS0}(\boldsymbol{\alpha}_{III})$ is approximately 4% of the nominal output values of SS0, which is almost the biggest variation observed in SS0. When the RTR is reduced to $\boldsymbol{\alpha}_{II} = [0.91\ \ 0.39\ \ 1]$, R_{SS0} $(\boldsymbol{\alpha}_{II})$ is reduced to 1.5% of the nominal output values. If the *RTR* is further reduced to $\boldsymbol{\alpha}_I$ (i.e., [0.02 0.78 0.96]), R_{SS0} $(\boldsymbol{\alpha}_I)$ is only about 0.9% of the nominal output values, which is the smallest variation observed in SS0 for this problem. The corresponding subsystem values are shown in "Appendix." Clearly, as *Investment* values are increasing in this procedure, we eliminate the amount of uncertainty in input parameters and outputs, as shown in Table 1.

In order to identify the relative importance of each uncertain parameter, a correlation plot of α_1, α_2, R and *Investment* for all Pareto $\boldsymbol{\alpha}$ solutions in Fig. 8 is given

Table 1 Typical α solutions, *investment* vs. R_{SS0}

	x_1	t_1	t_2	RSS0 (% of nominal)	*Investment*
α_I	0.02	0.78	0.96	0.86%	70%
α_{II}	0.91	0.39	1.00	1.49%	44%
α_{III}	0.99	0.99	1.00	3.94%	2%

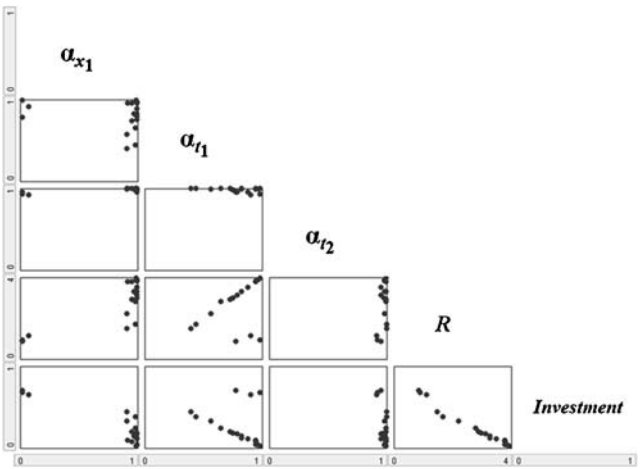

Fig. 9 Numerical example: plots of correlations among α, investment and R

Table 2 Numerical example, correlation coefficient matrix of Pareto solutions at system level

Correlation coefficient	α_{x_1}	α_{t_1}	α_{t_2}	R	*Investment*
α_{x_1}	1	–	–	–	–
α_{t_1}	−0.20	1	–	–	–
α_{t_2}	0.79	−0.33	1	–	–
R	0.78	0.45	0.54	1	−0.98
Investment	−0.87	−0.29	−0.64	−0.98	1

in Fig. 9. To clearly illustrate the correlation among obtained solutions in Fig. 8, correlation coefficient matrix values were calculated as defined in Section 2, for $\boldsymbol{\alpha}$, R, and *Investment* and are reported in Table 2. It can be shown from Fig. 9 and Table 2 that among x_1, t_1, and t_2, the variable x_1 has the strongest correlation to the variation in SS0's outputs and *Investment*.

The details of subsystem solutions corresponding to Fig. 8 are shown in Appendix. Several interesting observations can be concluded from Fig. 8 and Appendix: (1) The variations in all the subsystem level outputs and couplings are less than the specified AOVR and RTR of the target variables in each subsystem but the variation in SS1 is larger than the variation in SS2 as shown in Fig. 8b, c, showing that SS1 is more sensitive to the uncertainty; (2) Since we select the optimal solution from SS's Pareto with the minimum *Investment*, $\boldsymbol{\alpha}$ solutions from SS1 and SS2 are both large and near to 1, meaning only small amount of uncertainty need to be reduced in x_2 and x_3; (3) The variations in SS1's outputs are much larger than those in SS2's outputs, making it clear that the uncertainty in SS1 has a much greater effect on the variation in the system level outputs and since the variation in SS2's outputs is always much less than 1, the AOVR (± 5) for outputs in SS2 might be overestimated; iv) In both SS1 and SS2, the variation in the couplings, compared to their outputs, contributes significantly to each subsystem output variations; however, η_{C2}in SS2 is much smaller than 1 while most η_{C1} values are equal to 1 (i.e., the consistency constraint is active in SS1), meaning that the uncertainty propagated from SS2 to SS1 through the coupling variable t_2 makes more effect than the variation propagated to SS2 in t_1. All those observations can help the designers revise the settings of AOVR and TR of the target variable and bring them the insights to understand the uncertainty effect and its propagation in this bi-level multi-disciplinary problem.

4.2 Engineering example

To demonstrate the MIMOSA approach, a battery-powered right angle grinder model is chosen for its multi-disciplinary nature and its combination of continuous and discrete parameters. This angle grinder model was developed based on an all-at-once model first presented by Williams et al. (2008). Here, the Williams' model is decomposed into two coupled subsystem and a new battery subsystem is added, producing a bi-level multi-disciplinary system with three fully coupled subsystems. Figure 10 depicts a graphical overview of this new angle grinder model. The grinder system analysis models are collections of closed form equations, look-up tables and conditional functions used to described the various performance and constraint functions of the system as functions of geometric and performance parameters. Although the grinder model contains no complex analyses, such as finite element analysis, the system and subsystem analysis models are treated as "black-box" functions considering only inputs and outputs, which typically represent many engineering analysis models. The inclusion of more complex analysis examples would not change the MIMOSA approach beyond an obvious increase in the required computational effort.

The overall grinder system model (SS0) consists of three subsystems which define the design of the three main physical components of the power tool: a battery pack model (SS1) Anonymous (2005), an electric motor model (SS2) and a bevel gear assembly (SS3). The design of each of the three subsystems, as shown in Fig. 11, is accomplished through the use of various equations that describe the physics, performance and geometry of the specific subsystem. Additionally, each of the grinder's three subsystems is connected to other subsystems through coupling variables. For these reasons, this model provides a good platform for demonstrating the MIMOSA approach. Each of the subsystems is briefly described in the following paragraphs.

As shown in Fig. 11, at the system level, there are three design variables that are used by more than one

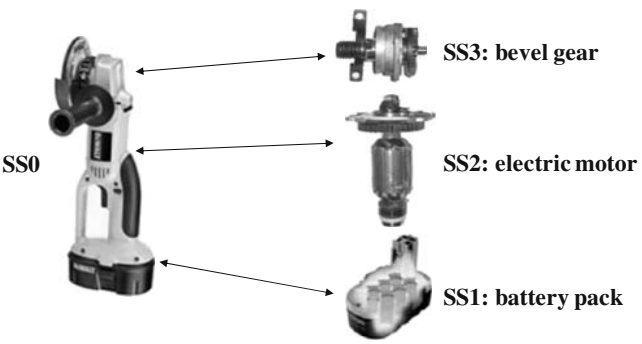

Fig. 10 Engineering example: right angle grinder

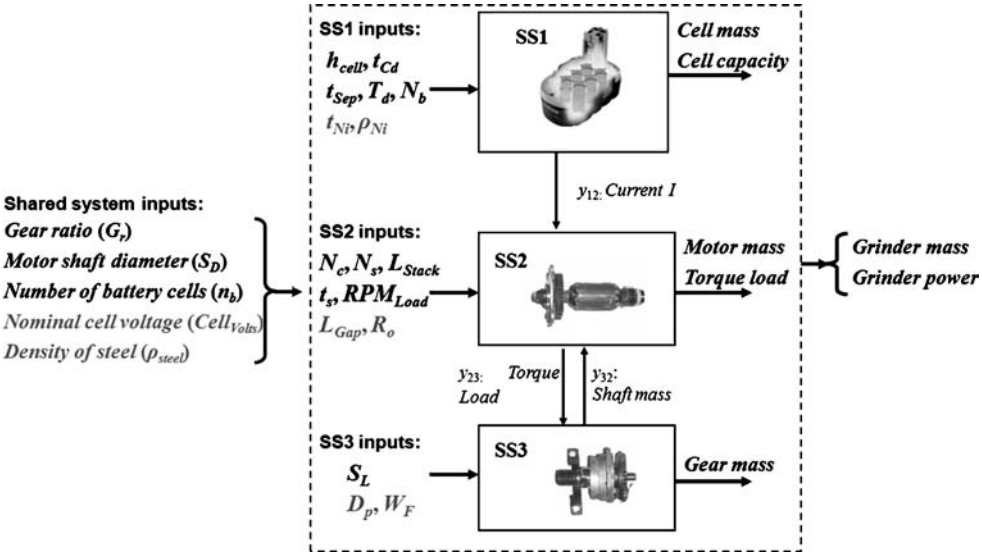

Fig. 11 Design variables, couplings, and outputs in grinder example

subsystem. These are gear ratio (G_r), motor shaft diameter (S_D), and number of battery cells in the battery pack (n_b), in which n_b is an integer variable. The overall system design outputs of interest are the total grinder mass and the total grinder power. Each subsystem has it own design variables and local outputs, as shown in Fig. 11. More importantly, there are three coupling variables that connect three subsystems: current (I) from SS1 to SS2, torque load from SS2 to SS3 and shaft mass from SS3 to SS2. In order to decompose the system into a decomposed framework, three target variables are introduced in SS0, one for each coupling. Thus, SS0 has six design variables in total. Two SS0's parameters have interval uncertainty in this example, as shown in Table 3. The design variables, parameters, and outputs of SS0 and each subsystem are detailed in the first column to the third column, respectively, in Tables 3, 4, 5, and 6, where a bold font is used to highlight the design variables or parameters which have interval uncertainty in SS0 and each subsystem. As discussed earlier in Section 3, the target variables must have an original tolerance region and a retained tolerance region controlled by their *PURI* vector. Additionally the outputs of interest in each subsystem have also been bolded, and will necessarily have resulting variation.

Each subsystem has its own design variables and parameters. For this study two parameters or design variables for each subsystem are assumed to have interval uncertainty, so there are two *PURI* values established in each subsystem to control the possible uncertainty level reduction. Each subsystem also has two outputs of interest, selected from their analysis outputs, except SS3 (Bevel Gear) which has only one output due to the relatively simple nature of the model. Tables 3, 4, 5, and 6 outlines the specifics of the four models that comprise the right angle grinder system.

In this engineering example, it is assumed that the designer does not have a specified AOVR for SS0 or subsystems and would like to understand the effects of input uncertainty on any possible variation ranges for the outputs at both system and subsystem levels. In this regard all output variations are normalized to their nominal output values and the MIMOSA formulation in (9) is used for each subsystem. A grinder design was obtained to serve as the nominal or candidate solution using the MOCO approach (Aute and Azarm 2006). Using this candidate design, a set of MIMOSA Pareto solutions is obtained using (6) and (9) at the system and subsystem levels with three typical solutions as shown in Fig. 12. Different from the numerical example, the optimal $\boldsymbol{\alpha}_i$ solution with the minimum R_{SSi} is selected from SSi's Pareto in this engineering example and used to calculate the outputs of the SA problem in SS0. The R_{SS0} is shown as a percentage of the nominal output function values. [α_1, α_2, α_3, α_4, α_5] is the *PURI* vector corresponding for [target current, target torque load, target shaft mass, cell volts, density of steel], as shown in bold in Table 3. The trade-off between *Investment* and the variation in SS0's outputs R_{SS0} are clearly shown in Fig. 12. Figure 13 shows the correlation plot figures for five *PURI* elements along with R_{SS0} and Investment_{SS0} for all Pareto $\boldsymbol{\alpha}$ solutions shown in Fig. 12. The correlation coefficient values for all Pareto $\boldsymbol{\alpha}$ solutions in Fig. 12 are also given in Table 7.

As shown in Fig. 12a, with the obtained largest uncertainty intervals ($\boldsymbol{\alpha}_{III}$ = [0.95 1.00 0.98 0.68 0.98]), the variations in SS0's outputs are about 6.2% of their nominal values. With more uncertainty being reduced

Table 3 Grinder system (SS0)

Grinder variables	Grinder parameters	Grinder outputs (units)
Number of battery cells (n_b)—integer	External components mass (m_{ext})	**Grinder mass (lbs)**
Gear ratio (G_r)	***Nominal cell voltage ($Cell_{Volts}$)***	Grinder RPMs (rpm)
Motor shaft diameter (S_D)	**Density of steel (ρ_{steel})**	Grinder current (A)
Target torque load		**Grinder power (W)**
Target shaft mass		Grinder duration (hr)
Target current		Grinder girth (in)

Table 4 Battery subsystem (SS1)

Battery variables	Battery parameters	Battery outputs (units)
Battery cell height (h_{cell})	Nominal NiCd cell voltage (V_{cell})	**Battery cell mass (lbs)**
Nickel reactant sheet thickness (t_{Ni})	**Density of nickel (ρ_{Ni})**	**Battery cell capacity (Ah)**
Cadmium reactant sheet thickness (t_{Cd})	Density of cadmium(ρ_{Cd})	Grinder voltage (V)
Separator sheet thickness (t_{Sep})	Density of separator material(ρ_{Sep})	Battery pack mass (lbs)
cell discharge time(T_d)	Density of cell wall material (ρ_{cw})	
Battery cell coil turns (N_b)—integer	Battery cell wall thickness (cwt)	

Table 5 Electric motor subsystem (SS2)

Motor variables	Motor parameters	Motor outputs (units)
Motor armature wire turns (N_c)—integer	Density of steel (ρ_{steel})	**Motor mass (lbs)**
Stator armature wire turns (N_s)—integer	Shear strength of steel (τ_{steel})	Motor girth (in)
Stator outer radius (R_o)	Density of copper (ρ_{Cu})	Motor RPM (rpm)
Stator thickness (t_S)	20 awg wire resistivity (R_w)	**Torque load (ft-lbs)**
Gap length (L_{Gap})	20 awg wire cross-section area (A_w)	
Stack length (L_{Stack})	Brush loss factor (α_{Brush})	
Grinder RPMs—loaded (RPM_{Load})	Permeability of free space (μ_O)	
	Permeability of steel (μ_{Steel})	

Table 6 Bevel gear subsystem (SS3)

Gear variables	Gear parameters	Gear outputs (units)
Motor shaft length (S_L)	Pressure angle (θ_P)	**Gear mass (lbs)**
Pinion pitch diameter (D_p)	**Face width (W_F)**	
	Gear elasticity factor (Z_e)	
	Amplification factor (K_a)	
	Load distribution factor (K_m)	
	Geometric factor (G_F)	
	Density of steel (ρ_{steel})	
	Arbor mass (m_A)	
	Commutator mass (m_C)	
	Pinion shaft mass (m_{PS})	

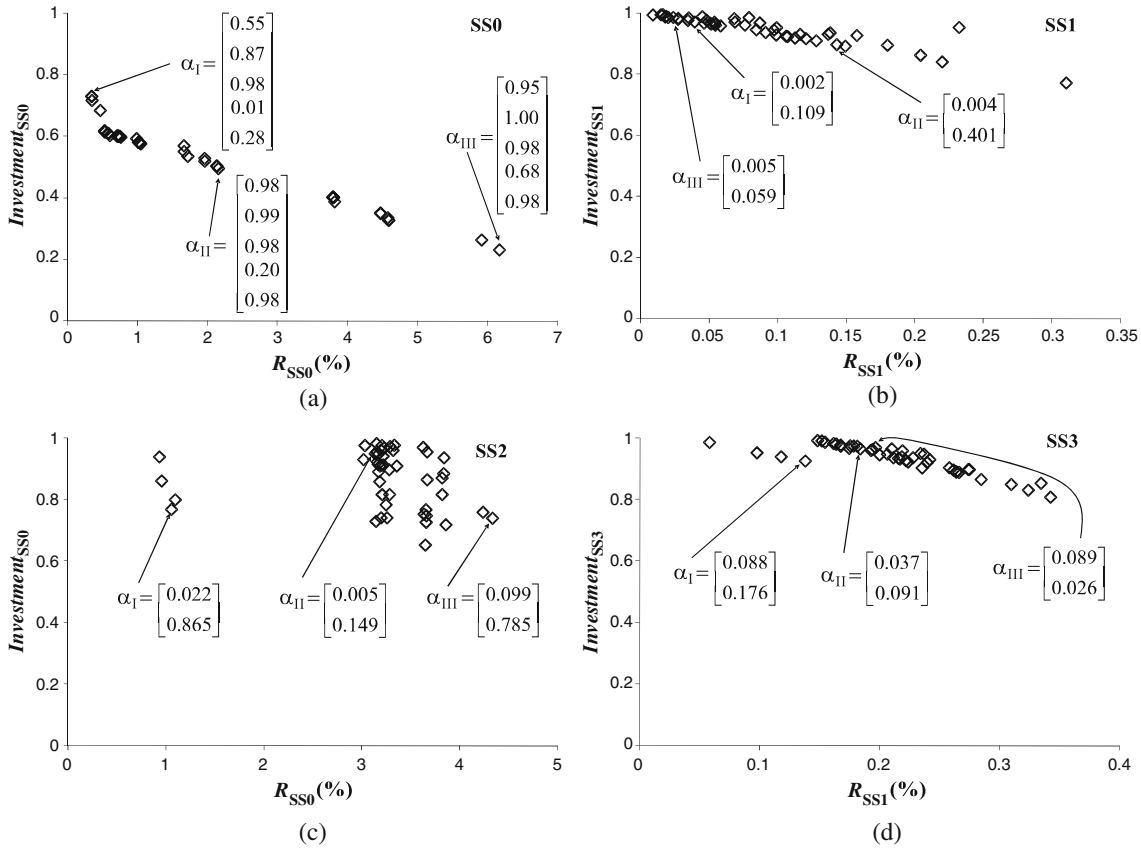

Fig. 12 Grinder design: Pareto solutions for system and subsystem levels: **a** SS0, **b** SS1, **c** SS2, and **d** SS3

(i.e., $\boldsymbol{\alpha}_I = [0.55\ 0.87\ 0.98\ 0.01\ 0.28]$), the R_{SS0} can be reduced to around 0.3% of the nominal value.

As clearly shown in Fig. 13 and Table 7 (in the grey cells), among those five uncertain parameters, Cell_{volts} (α_4) has the strongest, while target shaft mass has the weakest, correlation to the system output variation.

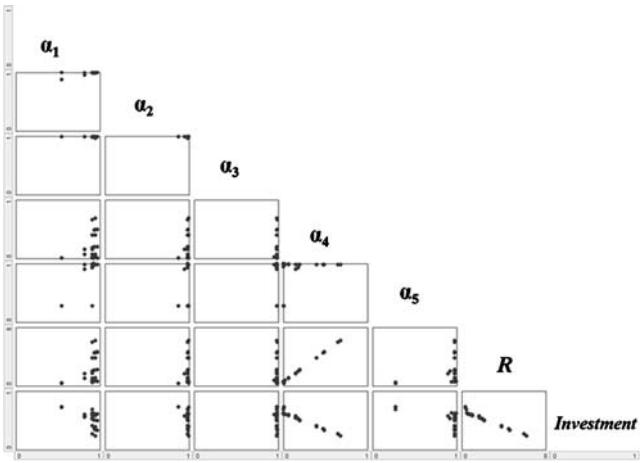

Fig. 13 Grinder design: plots of correlations among α, *investment* and R

Other three uncertain parameters are in the middle. In this regard, more investment should be used to reduce the uncertainty in the cell volts and the uncertainty in the current for the battery part (the second strongest correlated to R_{SS0}), which is consistent with our expectations since the voltage and output current of the battery can significantly affect the performance of the grinder.

Due to space limitations, detailed solutions from each of the subsystems are not given here. However, some additional observations are made in this example. Since a single optimal solution that possesses the minimum R_{SSi} from each subsystem's Pareto is selected for use in the corresponding SS0 solution, the *Investment* required by all three subsystems are relatively large, as shown in Fig. 12b–d. It is also observed that although all three subsystems have comparable variations in their mass values, after normalizing them by their nominal values, the normalized variation in SS2' outputs (Fig. 12c) is considerably larger than the variation in SS1 and SS3 (Fig. 12b, d). This shows that SS2 is more sensitive to the input uncertainty in this grinder model. The variations in the coupling variables are always less than the RTR of the target variables due to the

Table 7 Grinder design: correlation coefficient matrix of Pareto solutions at system level

Correlation coefficient	α_1	α_2	α_3	α_4	α_5	R	*Investment*
α_1	1	–	–	–	–	–	–
α_2	0.75	1	–	–	–	–	–
α_3	−0.18	−0.05	1	–	–	–	–
α_4	0.31	0.23	0.25	1	–	–	–
α_5	0.82	0.64	−0.19	0.29	1	–	–
R	0.34	0.25	0.24	1	0.32	1	−0.98
Investment	−0.51	−0.39	−0.19	−0.97	−0.50	−0.98	1

consistency constraint. Moreover, at the subsystem level, three uncertain parameters, the nickel reactant sheet thickness in SS1, the stator outer radius in SS2, and the pinion pitch diameter in SS3, compared to another uncertainty parameter in the corresponding subsystem, are more strongly correlated to the output variations in their subsystems. They have been italicized through Tables 4, 5, and 6. More investment should be spent on reducing uncertainty in those three parameters. This is an interesting finding recalling that in the current algorithm from the subsystem level the *PURI* vector values are selected in order to produce the greatest reduction in subsystem output variation (minimum R without regard for *Investment*). In the case of the battery subsystem, this choice clearly demonstrates that controlling the nickel reactant sheet thickness parameter is far more important than controlling the density of the nickel used to ensure the performance of the battery subsystem. Figure 14 is a plot of the corresponding *PURI* values for t_{Ni} and ρ_{Ni} from SS1 for all Pareto solutions at the system level shown in Fig. 12. As can be seen on the figure, the *PURI* values for t_{Ni} are much smaller than the corresponding *PURI* values for ρ_{Ni}, which indicate that in order to produce optimal variation reduction in the outputs for the battery subsystem, the uncertainty in the geometric parameter must be much more tightly controlled.

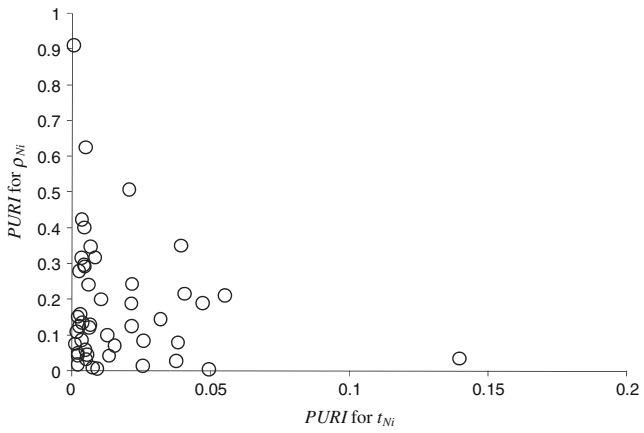

Fig. 14 *PURI* values of t_{Ni} and ρ_{Ni} for Pareto solutions at system level

Based on the data presented, in order to optimally reduce the variation in the outputs at the system and subsystem levels, the designer of this right angle grinder should reduce the uncertainty mainly in the four parameters (or design variables) which are italicized through Table 3 to Table 6. The results shown here, while clearly based on the grinder model used for this example, highlight the greater capability of the MIMOSA approach to efficiently identify the most important uncertain parameters in a complex model during the conceptual phase of design. This discussion is merely an example of the type of data that could be extracted from each of the other subsystems and how it might be analyzed.

5 Conclusions

In this paper a new global SA method, called MIMOSA, is presented. MIMOSA has the ability to analyze the effects of uncertainty on system and subsystem performance for fully coupled multi-output multi-disciplinary problems in which uncertainty exist not only in parameters in each subsystem but also in the subsystem couplings. Given multiple interval uncertainties for parameters at the system and subsystem levels, MIMOSA can optimally identify how much the investment is necessary to optimally reduce uncertainty in input parameters in order to ensure a desired level of variation in the system and subsystems' output values, considering a single design or a set of designs. Two metrics, R and *Investment*, have been used in the SA problems in SS0 and subsystems to quantify the variation in multiple system and/or subsystem outputs and the cost used to reduce the input uncertainty. MIMOSA can also efficiently determine the relative importance among uncertain parameters in the system and subsystems in terms of uncertainty reduction. Subsystems' relative importance, in terms of their contribution to the entire system performance variation, can also be analyzed using this new approach. MIMOSA is a global

Table 8 Numerical example: detailed value in SS1 and for Pareto solutions in Fig. 8

Solution #	α_{x_2}	$\max\left[R_{SS1}, \eta_{c_1}\right]$	$Investment_{SS1}$	η_{c_1}	$\Delta o_{1,1}$	$\Delta o_{1,2}$
1: α_I	0.996	0.306	0.004	0.306	0.648	0.165
2	0.992	0.237	0.008	0.237	0.628	0.16
3	0.985	0.314	0.015	0.314	0.839	0.214
4: α_{II}	0.99	1	0.01	1	1.273	0.329
5	0.959	1	0.041	1	1.444	0.373
6	0.996	1	0.004	1	1.969	0.494
7	1	1	0	1	2.302	0.569
8	0.996	1	0.004	1	2.625	0.646
9	0.982	1	0.018	1	2.717	0.662
10	0.859	1	0.141	1	2.849	0.699
11	0.998	1	0.002	1	3	0.728
12	0.998	1	0.002	1	3	0.735
13	0.984	1	0.016	1	3.215	0.779
14	0.998	1	0.002	1	3.5	0.834
15	1	1	0	1	3.5	0.838
16	1	1	0	1	3.5	0.84
17	0.969	1	0.031	1	3.591	0.851
18: α_{III}	1	1	0	1	3.637	0.865

SA approach which uses interval uncertainty to quantify the uncertainty instead of gradient information or probability density functions. Because MIMOSA is accomplished by using the MOGA as its optimization solver, it is capable of handling both continuous and discrete design variables and/or parameters. Finally, MIMOSA is flexible enough to be able to handle various designer preferences, including the limits on parameter uncertainty reduction levels, different acceptable output variation levels, and different selection strategies if applicable.

The applicability and capabilities of the MIMOSA approach have been demonstrated using a numerical and an engineering example, both of which have multiple fully coupled subsystems. The numerical example had two outputs in each of two subsystems while the engineering example includes three subsystems and has mixed continuous-discrete design variables. From the results obtained in these two examples, the trade-off between the investment used to reduce the uncertainty levels in the input parameters and the variations in the system outputs are clearly demonstrated. Both examples show the ability of MIMOSA to optimally determine the best uses of limited investment available for uncertainty reduction in the attempt to improve system performance in terms of reducing output variations. The correlation between uncertain parameters and the variations in the system and subsystem outputs are easily determined based on the obtained Pareto solutions for R vs. *Investment*. Both examples specifically present

Table 9 Numerical example: detailed value in SS2 and for Pareto solutions in Fig. 8

Solution #	α_{x_3}	$\max\left[R_{SS2}, \eta_{C_2}\right]$	$Investment_{SS2}$	η_{C_2}	$\Delta o_{2,1}$	$\Delta o_{2,2}$
1: α_I	0.948	0.112	0.052	0.112	0.217	0.006
2	0.896	0.145	0.104	0.145	0.29	0.006
3	0.968	0.143	0.032	0.143	0.281	0.026
4: α_{II}	0.889	0.153	0.111	0.153	0.216	0.299
5	0.933	0.166	0.067	0.166	0.231	0.324
6	0.979	0.177	0.021	0.177	0.239	0.3
7	0.999	0.199	0.001	0.199	0.49	0.324
8	0.889	0.198	0.111	0.198	0.266	0.314
9	0.951	0.209	0.049	0.209	0.273	0.327
10	0.951	0.218	0.049	0.218	0.277	0.328
11	0.971	0.214	0.029	0.214	0.278	0.32
12	0.85	0.212	0.15	0.212	0.283	0.327
13	0.97	0.23	0.03	0.23	0.287	0.328
14	0.952	0.223	0.048	0.223	0.291	0.314
15	0.997	0.219	0.003	0.219	0.287	0.302
16	0.896	0.23	0.104	0.23	0.296	0.327
17	0.995	0.233	0.005	0.233	0.297	0.327
18: α_{III}	0.962	0.231	0.038	0.231	0.299	0.327

how the MIMOSA approach can identify the subsystem in a decomposed multi-subsystem problem that is the most sensitive to the uncertainty and has the greatest effect on the system level performance under uncertainty. The engineering example also demonstrates how MIMOSA is capable of isolating parameters whose uncertainty greatly influence system and subsystem outputs in contrast to those who do not. The importance of parameters in each of the subsystems of the angle grinder has been identified as well.

The MIMOSA approach presented is adaptable to many different types of engineering problems and thus has a wide range of applications not specifically addressed in this paper. As a result of this flexibility, the MIMOSA approach is an excellent tool for clearly understanding and optimally eliminating the wide-spread effects of uncertainty in many different engineering design efforts based on designer preferences, limitations and/or goals. For instance, *Investment* could be further defined to include a real cost function associated with specific uncertainty reductions, and that cost function needs not be the same for all uncertain parameters within a problem (e.g., Acar et al. 2007; Kale and Haftka 2008). MIMOSA could also be used to ignore (redundant) design parameters or outputs from the design process that are unimportant or already insensitive to uncertainty in favor of using valuable computational resources for the more important or more critical design aspects, thus simplifying a complicated problem down to a more manageable size consisting of more relevant issues.

Acknowledgements The work presented in this paper was supported in part through a contract from the Office of Naval Research contract number N000140810047. Such support does not constitute an endorsement by the funding agency of the opinions expressed in the paper.

Appendix

The details of the Pareto solutions obtained for the numerical example are shown in this section, as in Tables 8 and 9.

References

Acar E, Haftka RT, Johnson TF (2007) Tradeoff of uncertainty reduction mechanisms for reducing weight of composite laminates. J Mech Des 129(3):266–274. doi:10.1115/1.2406097

Agarwal H, Renaud JE, Preston EL, Padmanabhan D (2004) Uncertainty quantification using evidence theory in multidisciplinary design optimization. Reliab Eng Syst Saf 85(1–3):281–294. doi:10.1016/j.ress.2004.03.017

Anonymous (2005) Bosch builds better bluecore battery. http://www.danshapiro.com/blog/archives/000171bosch_builds_better_bluecore_batteries.html. Accessed 14 Dec 2007

Aute V, Azarm S (2006) A genetic algorithms based approach for multidisciplinary multiobjective collaborative optimization. AIAA-2006-6953. In: Proceedings of the 11th AIAA/ISSMO Symposium on Multidisciplinary Analysis and Optimization Conference, Portsmouth, Virginia, Sep. 6–8

Chen W, Jin R, Sudjianto A (2005) Analytical variance-based global sensitivity analysis in simulation-based design under uncertainty. J Mech Des 127(5):875–886. doi:10.1115/1.1904642

Chiralaksanakul A, Mahadevan S (2007) Decoupled approach to multidisciplinary design optimization under uncertainty. Optim Eng 8(1):21–42. doi:10.1007/s11081-007-9014-2

Deb K (2001) Multiobjective optimization using evolutionary algorithms. Wiley, New York

Du X, Chen W (2002) Efficient uncertainty analysis methods for multidisciplinary robust design. AIAA J 40(3):545–552

Du X, Chen W (2005) Collaborative reliability analysis under the framework of multidisciplinary systems design. Optim Eng 6(1):63–84. doi:10.1023/B:OPTE.0000048537.35387.fa

Frey HC, Patil SR (2002) Identification and review of sensitivity analysis methods. Risk Anal 22(3):553–578. doi:10.1111/0272-4332.00039

Gu X, Renaud JE, Batill SM (1998) Investigation of multidisciplinary design subject to uncertainties. AIAA Paper 1998–4747. In: Proceedings of the 7th AIAA/ISSMO Symposium on Multidisciplinary Analysis and Optimization Conference, St. Louis, MO, Sep. 2–4

Gu X, Renaud JE, Penninger CL (2006) Implicit uncertainty propagation for robust collaborative optimization. J Mech Des 128(4):1001–1013. doi:10.1115/1.2205869

Hamby DM (1994) Review of techniques for parameter sensitivity analysis of environmental models. Environ Monit Assess 32(2):135–154. doi:10.1007/BF00547132

Helton JC, Davis FJ (2003) Latin hypercube sampling and the propagation of uncertainty in analyses of complex systems. Reliab Eng Syst Saf 81(1):23–69. doi:10.1016/S0951-8320(03)00058-9

Iman RL, Helton JC (1988) An investigation of uncertainty and sensitivity analysis techniques for computer models. Risk Anal 8(1):71–90. doi:10.1111/j.1539-6924.1988.tb01155.x

Kale AA, Haftka RT (2008) Tradeoff of weight and inspection cost in reliability-based structural optimization. J Aircr 45(1):77–85. doi:10.2514/1.21229

Kern D, Du X, Sudjianto A (2003) Forecasting manufacturing quality during design using process capability data. In: Proceedings of the IMECE' 03, ASME 2003 International Mechanical Engineering Congress and RD&D Expo, Washington, DC, Nov. 15–21

Kokkolaras M, Mourelatos ZP, Papalambros PY (2006) Design optimization of hierarchically decomposed multilevel systems under uncertainty. J Mech Des 128(2):503–508. doi:10.1115/1.2168470

Li M (2007) Robust optimization and sensitivity analysis with multi-objective genetic algorithms: single- and multi-disciplinary applications. Ph.D. Dissertation, University of Maryland, College Park, Maryland

Li M, Azarm S (2008) Multiobjective collaborative robust optimization (McRO) with interval uncertainty and interdisciplinary uncertainty propagation. J Mech Des 130(8):081402/1–081402/11. doi:10.1115/1.2936898

Li M, Williams N, Azarm S (2009) Interval uncertainty reduction and sensitivity analysis with multi-objective design optimization. J Mech Des 131(3):031007/1–031007/11. doi:10.1115/1.3066736

Noor AK, Starnes JH, Peters JM (2000) Uncertainty analysis of composite structures. Comput Methods Appl Mech Eng 185(2–4):413–432. doi:10.1016/S0045-7825(99)00269-8

Padula SL, Gumbert CR, Li W (2006) Aerospace applications of optimization under uncertainty. Optim Eng 7(3):317–328. doi:10.1007/s11081-006-9974-7

Qiu ZP, Ma Y, Wang XJ (2004) Comparison between non-probabilistic interval analysis method and probabilistic approach in static response problem of structures with uncertain-but-bounded parameters. Commun Numer Methods Eng 20:279–290. doi:10.1002/cnm.668

Rao SS, Cao LT (2002) Optimum design of mechanical systems involving interval parameters. J Mech Des 124(3):465–472. doi:10.1115/1.1479691

Saltelli A, Chan K, Scott EM (2000) Sensitivity analysis. Wiley, New York

Saltelli A, Ratto M, Andres T, Campolongo F, Cariboni J, Gatelli D, Saisana M, Tarantola S (2008) Global sensitivity analysis: the primer. Wiley, New York

Smith N, Mahadevan S (2005) Integrating system-level and component-level designs under uncertainty. J Spacecr Rockets 42:752–760

Sobieszczanski-Sobieski J (1990) Sensitivity of complex, internally coupled systems. AIAA J 28(1):153–160

Sobieszczanski-Sobieski J, Bloebaum C, Hajela P (1991) Sensitivity of control-augmented structure obtained by a system decomposition method. AIAA J 29(2):264–270

Sobol IM (2001) Global sensitivity indices for nonlinear mathematical models and their Monte Carlo estimates. Math Comput Simul 55(1–3):271–280. doi:10.1016/S0378-4754(00)00270-6

Williams N, Azarm S, Kannan PK (2008) Engineering product design optimization for retail channel acceptance. J Mech Des 130(6):061402/1–061402/10. doi:10.1115/1.2898874

Wu WD, Rao SS (2007) Uncertainty analysis and allocation of joint tolerances in robot manipulators based on interval analysis. Reliab Eng Syst Saf 92(1):54–64. doi:10.1016/j.ress.2005.11.009

Yin X, Chen W (2008) A hierarchical statistical sensitivity analysis method for complex engineering systems design. J Mech Des 130(7):071402/1–071402/10. doi:10.1115/1.2918913